P-ISSN: 2304-3075; E-ISSN: 2305-4360
International Journal of Veterinary Science
www.ijvets.com; editor@ijvets.com
Research Article DOI: 10.37422/IJVS/030

Role of Artesunate in Potentiation of β-lactam Against Methicillin Resistant *Staphylococcus aureus* (MRSA) Isolated from Bovine Mastitis and its Histopathology Impact In-Vivo Study

Mohamed K Elbayoumy[1], Ahmad M Allam[1], Shimaa T Omara[2,*], Elgabry A Elgabry[2], and Sherein S Abdelgayed[3]

[1]Parasitology and Animal Diseases dept., Veterinary Division, National Research Centre; [2]Microbiology and Immunology Department, National Research Centre, 33 Bohouth St. Dokki, Affiliation I.D. 60014618, Postal Code 12311, Giza, Egypt; [3]Pathology Department, Faculty of Veterinary Medicine, Cairo University, Egypt
***Corresponding author:** shimaa_omara2112@yahoo.com

Article History: 19-738 Received: December 18, 2019 Revised: February 25, 2020 Accepted: March 20, 2020

ABSTRACT

This article discusses the augmenting influence of Artesunate (ART) in combination with β-lactams (amoxicillin/clavulanic acid) antibiotic in sepsis mice models infected by a lethal challenge dose of live coagulase positive enterotoxigenic (*Sec*) MRSA that was isolated from a case of chronic bovine mastitis. The main goal is to find an appropriate treatment to overcome resistance mechanism of MRSA towards β-lactams antibiotic. Fifty healthy adult Swiss mice divided into 5 equal groups were used in the experimental procedure. The infected group that treated with both ART and β-lactams (amoxicillin/clavulanic acid) antibiotic revealed complete inhibition of MRSA count with complete normal macroscopic and histopathological features. We suggest that ART can potentiate the antibacterial action of β-lactams (amoxicillin/Clavulanic) acid against MRSA infection. The combination of ART and antibiotic can overcome MRSA resistance mechanism and so could be considered a novel candidate to overcome mastitis and/or sepsis caused by MRSA.

Key words: Mastitis, MRSA, β-lactam, Artesunate, Mice, Histopathology

INTRODUCTION

Mastitis is considered one of the most costly production diseases facing worldwide dairy industry (Dalanezi *et al.,* 2020). *Staphylococcus aureus* (*S. aureus*) is the main incriminated pathogen in bovine mastitis (Swarnakar *et al.,* 2017; Khazandi *et al.,* 2018). Nowadays, the public health impact of methicillin-resistant *S. aureus* (MRSA) associated with food producing animals has been increased (Basanisi *et al.,* 2017). Cows', small ruminants' milk and various dairy products were founded to be sources for MRSA infections (Ünal *et al.,* 2012).

The administration of antibiotics as growth promoters or their extensive therapeutic usage in the animal production, both were the main causative agents of the development of bacterial resistance (Yu *et al.,* 2017; Scott *et al.,* 2018). The dangerous of the development of antibiotic resistance as well as the high cost of antibiotic, make the antibiotic treatment unfavorable (Fluit, 2012).

Amoxicillin in combination with β-lactamase inhibitors (Synulox® LC, Pfizer) is potentially useful for the treatment of bovine mastitis caused by pathogenic organisms (Li *et al.,* 2014). However, to combat the bacterial resistance mechanism, there is a concept to apply a combination therapy composed of an antibiotic and another compound that enhance the antibiotic's activity (Ma *et al.,* 2017). Among these compounds, is Artesunate (ART) which is extracted from the Chinese herb Artemisia Annua and which is applied as an efficient treatment of malaria (WHO, 2001; Wu *et al.,* 2016). Notably, ART is an effective antiviral agent (EL-Bayoumy *et al.,* 2013).

This study aimed to study the effect of ART in combination with β-lactams (amoxicillin/clavulanic acid) antibiotics in sepsis mice models infected by a lethal challenge dose of live coagulase positive enterotoxigenic (*Sec*) MRSA strain that was isolated from a case of chronic bovine mastitis and to discuss the survival rate of the infected mice after treatment. Moreover, we aimed to study the ART's effects on the MRSA count within the internal organ as well as post-mortem and histopathological features.

Cite This Article as: Elbayoumy MK, AM Allam, ST Omara, EA Elgabry, SS Abdelgayed, 2020. Role of artesunate in potentiation of β-lactam against methicillin resistant *Staphylococcus aureus* (MRSA) isolated from bovine mastitis and its histopathology impact in-vivo study. Int J Vet Sci, 9(3): 337-342. www.ijvets.com

MATERIALS AND METHODS

MRSA strain

A coagulase positive enterotoxigenic (Sec) *S. aureus* MRSA strain that was previously isolated from a case of chronic bovine mastitis by Omara (2017) is used in the present study.

Enterotoxin extraction from *S. aureus*

The enterotoxin was extracted by sac cultural method according to Donnelly *et al.* (1967) and confirmed serologically by reversed passive latex agglutination kits (RPLA) (Oxoid) according the manufacturer's instructions. The identified MRSA bacterial isolate was stored in a brain heart infusion broth supplemented by 15% glycerol at −80°C and also streaked into BHI slants to be used for the mice injection.

Determination of the lethal bacterial dose

The lethal dose of *S. aureus* to mice was determined by mice I/P injection with 200 µl of variable numbers of the enterotoxigenic (*Sec*) *S. aureus* strain ranging from 1 X 10^2 to 4 X 10^{11} cells per dose according to Matsuzaki *et al.* (2003).

MRSA counting

The enumeration of MRSA bacterium was performed on the Baird-Parker agar medium (Oxoid) supplemented with egg yolk tellurite emulsion (SR0054, Oxoid) as follow, one gram of a pool of internal organs (liver, spleen, kidneys) of each mice was homogenized in 9 ml buffered peptone water in a sterile mortar, followed by tenfold serial dilution in a sterile buffered peptone water, 100 µl of each dilution were then inoculated in triplicate onto the surface of the Baird-Parker agar and evenly distributed by a sterile glass rod spreader. Plates were then left for one minute at ambient temperature and were incubated aerobically at 37°C for 24 h. Black colonies surrounded with opaque halo zone were counted as MRSA isolate and the MRSA CFU (Colony forming unit) was determined. These colonies were picked up, streaked on brain heart infusion agar (Oxoid), and microbiologically tested as mentioned before for confirmation.

Drugs and chemicals

ART (Sigma-Aldrich Chemie GmbH) was dissolved in 1mL of 5% sodium bicarbonate and was used in concentration of 30 mg/kg/day (Krishna *et al.*, 2001). Synulox™ (Zoetis) is a ready to use injection, each ml contains 140 mg Amoxicillin (as amoxicillin trihydrate; a β–lactam antibiotic) and 35 mg Clavulanic acid (as potassium clavulanate, a β–lactamase inhibitor).

Lab animal experimental procedure

A total of 50 adult female albino Swiss mice (~20±2g) were obtained from the National Research Centre (NRC), Cairo-Egypt and housed in a ventilated room with a 12 h light-dark cycle (22±1ºC, 60%±10% relative humidity).

Animals were randomly divided into five equal groups (A, B, C, D and E): group A represented the uninfected normal control group; received intraperitoneal (I.P.) injection of daily dose of 30 mg/kg of ART for 5 days. Group B represented the infected untreated group; received one I.P. injection of 200µl of MRSA strain in concentration of 1 X 10^{11} cells in the 1st day. Group C represented the infected group that received the ART; I.P. injection of daily doses of 30 mg/kg of ART for 5 days to assess its in vivo efficacy then received one I.P. injection of 200µl of the MRSA strain in concentration of 1 X 10^{11} cells in the 5th day. Group D represented the infected group that received both the ART and the antibiotic; received I.P. injection of daily doses of 30 mg/kg of ART for 5 days to assess its in vivo efficacy then received one I.P. injection of 200µl of the MRSA strain in concentration of 1 X 10^{11} cells in the 5th day followed by intramuscular (I.M.) injection of Synulox in a dose of 100mg/kg /12h for three days. Group E represented the infected group that treated by the antibiotic; received one I.P. injection of 200µl of the MRSA strain in concentration of 1 X 10^{11} cells in the 1st day followed by I.M. injection of Synulox in the same dose of previous group (D). All groups were noticed daily for recording any abnormalities and mortalities. At the end of the experiments, all mice were sacrificed for the post mortem study.

Histopathological examination

At necropsy, tissue samples of the heart, lung, liver, kidneys, spleen, and intestine from sacrificed mice in groups treated with ART alone or in combination with the antibiotic as well as the control positive infected group, all were collected and fixed in 10% neutral buffered formalin. Paraffin tissue sections at 4-6µ thickness were prepared and stained with hematoxylin and eosin for histopathological examination (Bancfort and Stevens, 1996).

Statistical analysis

The statistical analysis of MRSA counts (CFU/gm) in each mice group was represented in terms of Mean, Standard Deviation and One-way ANOVA.

RESULTS

Determination of lethal bacterial challenge dose

The intra-peritoneal injections of 1 X 10^2 to 4 X 10^{10} did not decrease the survival rate within the following 7-day observation period. By contrast, injections of 6 X 10^{10} - 4 X 10^{11} cells dropped the survival rate in a dose-dependent manner. Injection of 1 X 10^{11} cells killed 70% of mice within 24 h and 100% within 7 days of injection, this level of challenge was considered to be ideal for discussing the ART effect on bacterial lethality (Fig. 1). Therefore, the lethal challenge dose of *S. aureus* was fixed at 1X 10^{11} cells throughout the experiment.

A more precise time-chase analysis showed that, I.P injection of 1 X 10^{11} cells killed most mice 6-7 hours after injection, accompanied with preceding bacteremia. Postmortem examination of mice that died from bacterial infection after injection revealed severe general congestion; the pathological investigation of dead mice due to severe bacteremia is presented in Fig. 2. It revealed dilatation and congestion of the myocardial blood vessels in heart muscle cells (Fig. 2a), dilatation of the peribronchial blood vessel with peribronchial and perivascular mononuclear cells infiltrations in lung tissue (Fig. 2b),

Fig. 1: Determination of the challenge lethal dose of *S. aureus* to mice: serially diluted suspensions of bacterial cells were injected I.P. into mice. The mice fatalities were observed.

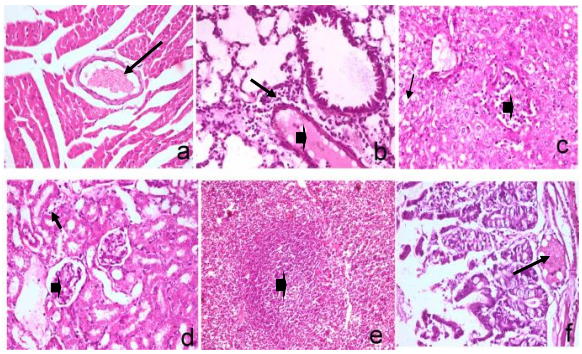

Fig. 2: Dead mice due to severe *S. aureus* bacteremia: (a) Heart showing dilatation and congestion of the myocardial blood vessels (arrow), (b) Lung showing dilatation of the peribronchial blood vessel (arrow head) with peribronchial and perivascular mononuclear cells infiltrations (arrow), (c) Liver showing vacuolarly degenerated hepatocytes (arrow) and focal area of necrosed hepatocytes infiltrated with leucocytic cells (arrow head), (d) Kidneys showing vacuolated glomerular tuft epithelium (arrow head) and renal tubular epithelium (arrow), (e) Spleen showing depletion of the splenic follicles (arrow head), (f) Intestine showing submucosal congestion of the blood vessel (arrow), (H&E X 200).

Table 1: Mean MRSA counts (CFU/gm) detected in the five groups of mice.

10 mice in each group	Mice Groups				
	A	B	C	D	E
1	0	42000x10^2	3x10^2	0	160x10^2
2	0	65000x10^2	1x10^2	0	170x10^2
3	0	53000x10^2	2x10^2	0	160x10^2
4	0	45000x10^2	1x10^2	0	180x10^2
5	0	55000x10^2	2x10^2	0	160x10^2
6	0	56000x10^2	3x10^2	0	170x10^2
7	0	64000x10^2	1x10^2	0	170x10^2
8	0	40000x10^2	3x10^2	0	160x10^2
9	0	52000x10^2	2x10^2	0	180x10^2
10	0	58000x10^2	2x10^2	0	190x10^2
Mean CFU/gm	0.00	5.30E+06	200.00	0.00	1.70E+04
SD	0.00	8.55E+05	81.65	0.00	1.05E+03
Minimum	0.00	4.00E+06	100.00	0.00	1.60E+04
Maximum	0.00	6.50E+06	300.00	0.00	1.90E+04
Median	0.00	5.40E+06	200.00	0.00	1.70E+04
IQR	0.00	1.52E+06	200.00	0.00	2.00E+03
P value [a]			0.001		
P value [b]		0.001	0.001	1.000	0.001

[a] P: Value between all groups using Non-parametric test (Kruskal-Wallis) test: [b] P: Value between each group and the control group (Group A) using Non-parametric test (Mann-Whitney) test: SD: Standard deviation: IQR: Interquartile range.

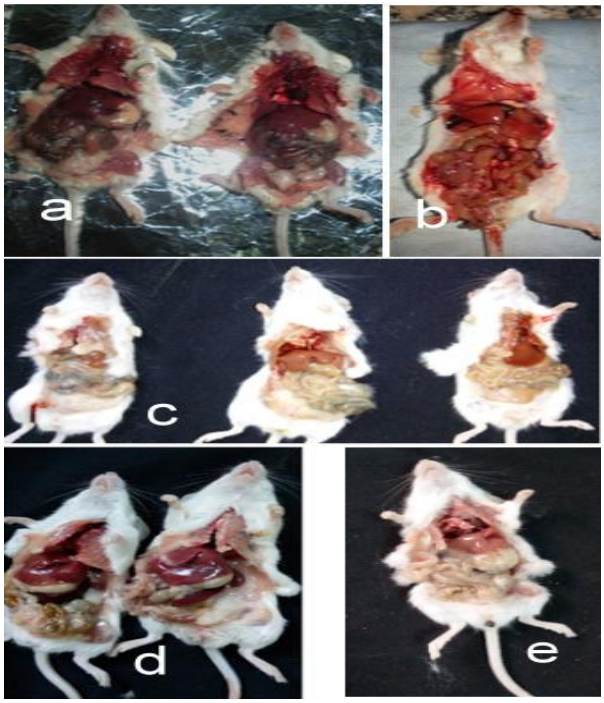

Fig. 3: (a) Uninfected normal control mice. (b) Infected untreated control mice. (c) Mice treated with Artesunate. (d) Mice treated with Artesunate and Synulox. (e) Mice treated with Synulox.

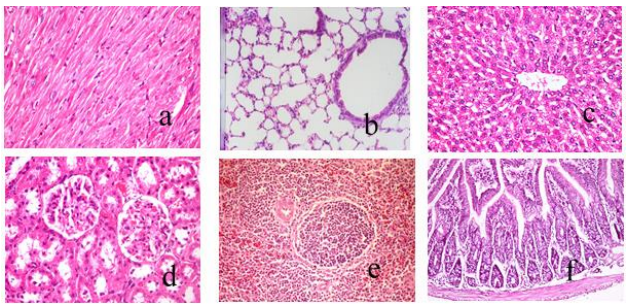

Fig. 4: Group A; Artesunate treated group: a- Heart showing normal myocardial muscle (H&E X 400):b- Lung showing apparently normal lung bronchi and alveoli (H&E X 400): c- Liver showing normal hepatocytes, portal tract, and blood sinusoids (H&E X 400): d- Kidneys showing normal renal glomeruli and renal tubules (H&E X 400): e- Spleen showing normal splenic follicles (H&E X 200): f- Intestine showing normal mucosa and submucosa (H&E X 200).

vacuolarly degenerated hepatocytes and focal area of necrosed hepatocytes infiltrated with leucocytic cells in liver (Fig. 2c), vacuolated glomerular tuft epithelium and renal tubular epithelium in kidneys (Fig. 2d), depletion of the splenic follicles in spleen (Fig. 2e), and submucosal congestion of the blood vessel in intestine (Fig. 2f).

Postmortem gross examination

The postmortem (PM) Gross Examination of group B revealed sever hemorrhage of the internal organs (Fig. 3b), while there were not any macroscopic alterations in other groups as presented in Fig. 3a, c, d & e.

MRSA count

The variations in the mean values of MRSA counts (CFU/gm) within the internal organs of mice in each

group are represented in Table 1. It can be clearly seen that group B had the highest mean MRSA count which dropped in groups C and E while both group A and D did not show any bacterial counts. The statistically analysis showed very high significance between the mice groups with general P value <0.05.

Histopathological results

Histopathology revealed considerable tissue damages caused by *S. aureus*. Yet it showed how the ART reduced the damage in different tissues. Microscopic examination of Group A revealed normal histology of all examined organs (heart, lung, liver, kidneys, spleen, and intestine) as presented in Fig. 4a, b, c, d, e and f respectively.

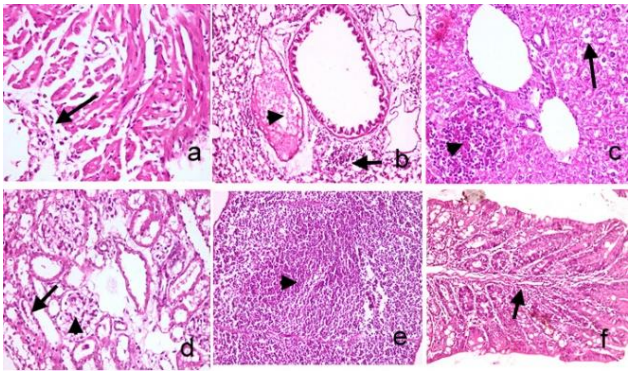

Fig. 5: Group B; *S.aureus* infected group: a- Heart showing myocardial hyalinosis together with mononuclear cells infiltrations (arrow), (H&E X 400): b- Lung showing bronchoectasia, with peribronchial congested blood vessels (arrow head) and leucocytic cells infiltrations (arrow) (H&E X 400): c- Liver showing vacuolarly degenerated hepatocytes (arrow) and focal area of necrosed hepatocytes infiltrated with leucocytic cells (arrow head), (H&E X 400): d- Kidneys showing vacuolated glomerular tuft epithelium (arrow head) and renal tubular epithelium (arrow), (H&E X 400): e- Spleen showing depletion of the splenic follicles (arrow head), (H&E X 400): f- Intestine showing diffuse infiltrations of the lamina propria with mononuclear cells (arrows), (H&E X 200).

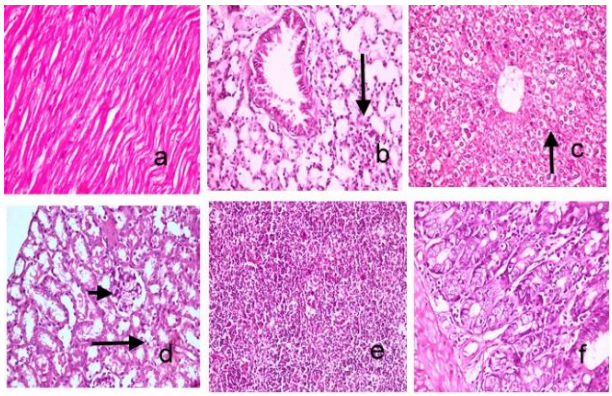

Fig. 6: Group C; treated with Artesunate then infected with *S. aureus*: a- Heart showing normal myocardial muscle (H&E X 400): b- Lung showing mild interstitial inflammatory reaction (arrow) (H&E x 400): c- Liver showing vacuolarly degenerated hepatocytes (arrow) with compressed blood sinusoids (H&E X 400): d- Kidneys showing vacuolated glomerular tuft epithelium (arrow head) and renal tubular epithelium (arrow), (H&E X 400): e- Spleen showing normal splenic follicles (H&E X 400): f- Intestine showing normal mucosa and submucosa (H&E X 400).

Microscopic alterations from Group B showed myocardial hyalinosis together with mononuclear cells infiltrations in heart (Fig. 5a), bronchoectasia, with peribronchial congested blood vessels and leucocytic cells infiltrations in lung (Fig. 5b). Vacuolarly degenerated hepatocytes and focal area of necrosed hepatocytes infiltrated with leucocytic cells in liver (Fig. 5c), vacuolated glomerular tuft epithelium and renal tubular epithelium in kidneys (Fig. 5d), depletion of the splenic follicles in spleen (Fig. 5e), and diffuse infiltrations of the lamina propria with mononuclear cells (Fig. 5f). Regarding Group C revealed normal heart muscle tissue (Fig. 6a), mild lung interstitial inflammatory reaction (Fig. 6b), mild vacuolarly degenerated liver hepatocytes (Fig. 6c), vacuolated kidney glomerular tuft epithelium and renal tubular epithelium (Fig. 6d), normal splenic follicles (Fig. 6e), and normal intestinal mucosa and submucosa (Fig. 6f). Microscopic examination of Group D; showed apparently normal tissue histology of all examined organs (heart, lung, liver, kidneys, spleen, and intestine) (Fig. 7a, b, c, d, e and f respectively).

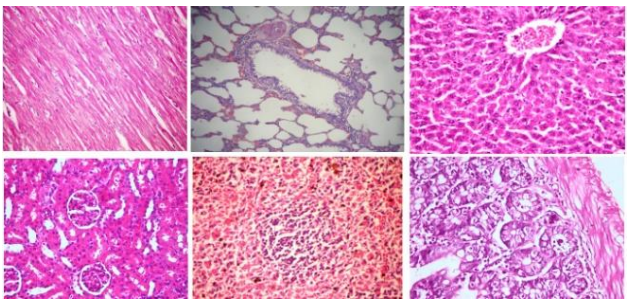

Fig. 7: Group D; infected with *S.aureus* then treated with Synulox and Artesunate: a- Heart showing normal myocardial muscle (H&E X 400): b- Lung showing apparently normal lung bronchi and alveoli (H&E X 400): c- Liver showing normal hepatocytes, portal tract, and blood sinusoids (H&E X 400): d- Kidneys showing normal renal glomeruli and renal tubules (H&E X 400): e- Spleen showing normal splenic follicles (H&E X 400): f- Intestine showing normal mucosa and submucosa (H&E X 400).

DISCUSSION

Nowadays drugs are quickly falling back in front of resistant mechanisms of MRSA. So currently it is urgent to develop a safe, effective, cheaper, and affordable drug for the treatment of MRSA. The main MRSA resistance mechanism against β-lactams antibiotic is via possession of penicillin-binding protein 2a (PBP2a), which its expression is via *mecA* gene. With MRSA, the β-lactams can block the Penicillin-binding proteins (PBPs), however the PBP2a could then replace the blocked PBPs. And so the bacterial growth will be maintained. Therefore, blocking PBP2a is supposed to be an amazing strategy to control MRSA infection (Jiang *et al.*, 2011).

Synulox™® is a combination treatment consisting of amoxicillin trihydrate (β-lactam antibiotic) and potassium clavulanate (β–lactamase inhibitor). This combination results in a new antibiotic with a broad antibacterial spectrum which is useful in overcoming amoxicillin-resistant β-lactamase producing bacteria. However, we are now searching for new agents that are able to produce a synergistic effect with the β-lactams in order to overcome

MRSA infection. Among these agents, ART is highlighted.

In this study a lethal challenge dose of live coagulase positive enterotoxigenic (Sec) MRSA strain (that was isolated from a case of chronic bovine mastitis) was used to induce sepsis in mice models. Our results demonstrated that only ART in combination with β-lactams (amoxicillin/clavulanic acid) could protect the survival rates of the experimentally infected mice with complete inhibition of MRSA count within the internal organs as well as complete normal macroscopic and histopathological feature.

Moreover, results in terms of histopathology view showed that the treated group by both ART and amoxicillin/clavulanic acid antibiotic showed rather normal picture compared to other groups which showed abnormalities with infiltration of mononuclear and leucocytic cells. Meanwhile, neither ART nor the amoxicillin/clavulanic acid antibiotics alone can neither protect nor treat the infected mice completely. Mice infected with *S. aureus* showed severe histopathological changes in their tissues (Braff *et al.,* 2007). *S. aureus* elicits marked alterations in the airways during pneumonia, including an increase in antimicrobial peptides, pro-inflammatory mediators, and coagulation proteins (Franklin and Lowy, 1998).

A previous study revealed that ART or β-lactam oxacillin drug alone was ineffective in the treatment of MRSA-infected mice (Jiang *et al.,* 2011; Ho *et al.,* 2014). However, ampicillin sodium–sulbactam sodium (AMPS) in combination with ART was found to be highly effective against lethal challenge doses of live *S. aureus* and could protect the survival rates of the infected mice better than the effect of the AMPS alone (Li *et al.,* 2010; Ho *et al.,* 2014). This means that, the ART does not have antibacterial effect but has β-lactams potentiating effect. Indeed, the FIC (fractional inhibitory concentration indexes) of ART in combination with a β-lactam drug were less than 0.5, which means presence of synergistic effect between both of them (Jiang *et al.,* 2011).

The synergistic potentiating mechanism between ART and β-lactam antibiotic can be explained as follows: when we treat MRSA by ART only, the ART will then bound to PBP2a which will in turn stops its function. However, the other PBPs cannot be blocked and still work well. And so MRSA could maintain live. On the other hand, when we use a combination treatment composed of both β-lactams and ART to overcome MRSA, the PBPs were then be blocked by β-lactams. In addition, PBP2a will be blocked by ART, so both of the PBPs and PBP2a will be blocked and so their functions will terminate and so the final result will be the bacterial death. Moreover, it has been reported that the synergistic potentiating mechanism between ART and oxacillin against lethal challenge dose of live MRSA was via decreasing the level of bacterial load, TNF-α (Tumor Necrosis Factor-α), and IL-6 (Interleukin-6) levels as previously recorded by Jiang *et al.,* 2011, behind the inhibition of multidrug efflux pump system (Li *et al.,* 2011).

Furthermore, the direct anti-inflammatory effect of ART is a very important factor against MRSA. This is due to prevention of the release of Nod2 (Nucleotide-binding oligomerization domain-containing protein 2)- mediated pro-inflammatory cytokines, TLR2 (Toll-like receptor 2), and TLR9 (Toll-like receptor 9) mRNAs (Messenger RNA) (Jiang *et al.,* 2011). Indeed, the powerful anti-inflammatory effects of ART is due to suppression of the release of Th-1 (T helper cells Type 1), Th-17 (T helper cells Type 17) cytokines, TNF-α, IL-6, and IFN-γ (Interferon gamma) through blocking of NF-κB (Nuclear factor kappa-light-chain-enhancer of activated B cells), TLR2, and Nod-2 activation (Li *et al.,* 2010; Ho *et al.,* 2014). Moreover, in case of bacterial infections ART can produce an immunomodulatory effect by modulating TLR2 and TLR9 pathways (Canivet *et al.,* 2015). In addition, ART was able to inhibit the infiltration of the inflammatory cell, MCP-1 (Monocyte chemoattractant protein-1), TNF-α, nitric oxide (NO), and aeroallergen neutrophil (Ho *et al.,* 2014).

Additionally, ART works by impairing the activation of host macrophages; preventing the production of the lethal NO and restoring normal NO production (Loo *et al.,* 2017). Furthermore, ART can act as a synergist for the antibiotic via inhibition of the dangerous H_2O_2 burst (Zeng *et al.,* 2011). Moreover, ART has the ability to prevent the expression of catalase, superoxide dismutases, and NADPH oxidases through the induction of nuclear factor (Ho *et al.,* 2014). Finally, the main powerful advantage of using ART in the treatment is that ART transforms quickly to its primary metabolite dihydroartemisinin which quickly comes out of the body (elimination half- life generally <1 h) (Vlietinck *et al.,* 2015).

Conclusions

In conclusion, our results demonstrated that ART in combination with β-lactams (amoxicillin/clavulanic acid) antibiotics is a novel candidate which can be used to overcome infection caused by MRSA like mastitis or sepsis. Further study to develop a product containing ART in combination with β-lactams (amoxicillin/clavulanic acid) antibiotic as a treatment to control bovine mastitis caused by *S. aureus* is required.

Author contributions

The authors participated in completing that work and approve the manuscript.

REFERENCES

Bancfort JD, Stevens A, 1996. Theory and practice of histological technique. 4 ed., New York: Churchill Livingstone.

Basanisi MG, La Bella G, Nobili G, *et al*., 2017. Genotyping of methicillin-resistant *Staphylococcus aureus* (MRSA) isolated from milk and dairy products in South Italy. Food Microbiol, 62: 141-146.

Braff MH, Jones AL, Skerrett SJ, *et al*., 2007. *Staphylococcus aureus* exploits cathelicidin antimicrobial peptides produced during early pneumonia to promote staphylokinase-dependent fibrinolysis. J Infec Dis, 195: 1365-72.

Canivet C, Menasria R, Rhéaume C, *et al*., 2015. Valacyclovir combined with Artesunate or rapamycin improves the outcome of herpes simplex virus encephalitis in mice compared to antiviral therapy alone. Antiviral Res, 123: 105-113.

Dalanezi FM, Joaquim SF, Guimarães FF, *et al*., 2020. Influence of pathogens causing clinical mastitis on reproductive variables of dairy cows. Journal of Dairy Science, Available online 20 February 2020, In Press, Corrected Proof.

Donnelly CB, Leslie JE, Black LA, *et al*., 1967. Serological identification of enterotoxigenic staphylococci from Cheese. Appl Microbiol, 15: 1382-1387.

EL-Bayoumy MK, Abdelrahman KA, Elgayed SS, *et al*., 2013. Antiviral Competence of Broad-Spectrum Antiinfective Drug Artesunate against Bovine Herpesvirus-1. Intl J Basic Appl Virol, 2: 06-13.

Fluit AC, 2012. Livestock-associated *Staphylococcus aureus.* Clin Microbiol Infec, 18: 735-744.

Franklin D and Lowy MD, 1998. *Staphylococcus aureus* Infections. N Eng J Med. 339: 520-532.

Ho WE, Peh HY, Chan TK and Wong WSF, 2014. Artemisinins: Pharmacological actions beyond anti-malarial. Pharmacol Therap, 142: 126-139.

Jiang W, Li B, Zheng X, *et al*., 2011. Artesunate in combination with oxacillin protect sepsis model mice challenged with lethal live methicillin-resistant *Staphylococcus aureus* (MRSA) via its inhibition on proinflammatory cytokines release and enhancement on antibacterial activity of oxacillin. Int Immunopharmacol, 11: 1065-1073.

Khazandi M, Al-Farha A, Coombs GW, *et al*., 2018. Genomic characterization of coagulase-negative staphylococci including methicillin-resistant *Staphylococcus sciuri* causing bovine mastitis. Veterinary Microbiology. 219: 17-22.

Krishna S, Planche T, Agbenyega T, *et al*., 2001. Bioavailability and preliminary clinical efficacy of intrarectal Artesunate in Ghanaian children with moderate malaria. Antimicrob. Agents Chemother, 45: 509-516.

Li B, Li J, Pan X, *et al*., 2010. ART protects sepsis model mice challenged with *Staphylococcus aureus* by decreasing TNF-alpha release via inhibition TLR2 and Nod2 mRNA expressions and transcription factor NF-kappaB activation. Int Immunopharmacol, 10: 344-350.

Li B, Yao Q, Pan XC, *et al*., 2011. Artesunate enhances the antibacterial effect of β-lactam antibiotics against *Escherichia coli* by increasing antibiotic accumulation via inhibition of the multidrug efflux pump system AcrAB-TolC. J Antimicrob Chemother, 66: 769-777.

Li H, Wu GQ, Tang SS, *et al*., 2014. Pharmacokinetics and pharmacodynamics of a novel amoxicillin/sulbactam/ prednisolone intramammary infusion in lactating cows after repeated administrations. Veterinarni Medicina, 59: 221-229.

Loo CSN, Lam NSK, Yu D, *et al*., 2017. Artemisinin and its derivatives in treating protozoan infections beyond malaria. Pharmacol Res, 117: 192-217.

Ma L, Wu J, Wang S, *et al*., 2017. Synergistic antibacterial effect of Bi2S3 nanospheres combined with ineffective antibiotic gentamicin against methicillin-resistant *Staphylococcus aureus.* J Inorg Biochem, 168: 38-45.

Matsuzaki S, Yasuda M, Nishikawa H, *et al*., 2003. Experimental Protection of Mice against Lethal *Staphylococcus aureus* Infection by Novel Bacteriophage. J Infec Dis, 187: 613-624.

Omara ST, 2017. MIC and MBC of Honey and Gold Nanoparticles against methicillin-resistant (MRSA) and vancomycin-resistant (VRSA) coagulase-positive S. aureus isolated from contagious Bovine clinical Mastitis. J Gen Engineer Biotechnol, 15: 219-230.

Scott AM, Beller E, Glasziou P, *et al*., 2018. Is antimicrobial administration to food animals a direct threat to human health? A rapid systematic review. Int J Antimicrob Agents, 04: 005.

SwarnakarG, D Sharma and Goswami H, 2017. Biofilm formation, hemolysin production and antimicrobial susceptibilities of Staphylococcus aureus isolated from the mastitis milk of buffaloes in Udaipur, India. Inter J Vet Sci, 6: 1-6.

Ünal N, Askar Ş, Macun H, *et al*., 2012. Panton-Valentine leukocidin and some exotoxins of *Staphylococcus aureus* and antimicrobial susceptibility profiles of staphylococci isolated from milks of small ruminants. Trop Anim Health Prod, 44: 573-579.

Vlietinck AJ, Pieters L, Apers S, *et al*., 2015. The value of central-African traditional medicine for lead finding: Some case studies. J Ethnopharmacol, 174: 607-617.

WHO, 2001. Guidelines Approved by the Guidelines Review Committee, Guidelines for the Treatment of Malaria, World Health Organization, Geneva.

Wu Y, Zhang L, W Li, *et al*., 2016. Artesunate restores spatial learning of rats with hepatic encephalopathy by inhibiting ammonia-induced oxidative damage in neurons and dysfunction of glutamate signaling in astroglial cells. Biomed Pharmacother, 84: 972-978.

Yu Z, Gunn L, Wall P, *et al*., 2017. Antimicrobial resistance and its association with tolerance to heavy metals in agriculture production. Food Microbiol, 64: 23-32.

Zeng QP, Xiao N, Wu P, *et al*., 2011. Artesunate potentiates antibiotics by inactivating heme-harbouring bacterial nitric oxide synthase and catalase. BMC Res Notes 30, 4-nthase and catalase. BMC Res Notes, 30: 4-223.